Available online at www.sciencedirect.com
SCIENCE DIRECT
Developmental Biology 295 (2006) 486–497
DEVELOPMENTAL BIOLOGY
www.elsevier.com/locate/ydbio

Cardiac arterial pole alignment is sensitive to FGF8 signaling in the pharynx

Mary R. Hutson *, Ping Zhang, Harriett A. Stadt, Asako K. Sato, Yin-Xiong Li [1], Jarrett Burch [2], Tony L. Creazzo, Margaret L. Kirby

Neonatal-Perinatal Research Institute, Division of Neonatology, Department of Pediatrics, Box 3179, Duke University Medical Center, Durham, NC 27710, USA

Received for publication 13 January 2006; revised 21 February 2006; accepted 27 February 2006
Available online 12 June 2006

Abstract

Morphogenesis of the cardiac arterial pole is dependent on addition of myocardium and smooth muscle from the secondary heart field and septation by cardiac neural crest cells. Cardiac neural crest ablation results in persistent truncus arteriosus and failure of addition of myocardium from the secondary heart field leading to malalignment of the arterial pole with the ventricles. Previously, we have shown that elevated FGF signaling after neural crest ablation causes depressed Ca^{2+} transients in the primary heart tube. We hypothesized that neural crest ablation results in elevated FGF8 signaling in the caudal pharynx that disrupts secondary heart field development. In this study, we show that FGF8 signaling is elevated in the caudal pharynx after cardiac neural crest ablation. In addition, treatment of cardiac neural crest-ablated embryos with FGF8b blocking antibody or an FGF receptor blocker rescues secondary heart field myocardial development in a time- and dose-dependent manner. Interestingly, reduction of FGF8 signaling in normal embryos disrupts myocardial secondary heart field development, resulting in arterial pole malalignment. These results indicate that the secondary heart field myocardium is particularly sensitive to FGF8 signaling for normal conotruncal development, and further, that cardiac neural crest cells modulate FGF8 signaling in the caudal pharynx.

Keywords: Heart development; FGF8, outflow tract; Arterial pole; Cardiac neural crest; Secondary heart field; Double outlet right ventricle; Persistent truncus arteriosus; Calcium transient; mkp3

Introduction

Development of the arterial pole of the 4-chambered heart requires complex morphogenetic movements to establish a single vascular channel with a myocardial-to-vascular smooth muscle interface. This single vascular channel is later divided into two outflow vessels by the cardiac neural crest cells (CNC). Finally, the two outflow vessels are remodeled to align them with the right and left ventricles.

The secondary heart field (SHF) has recently been shown to provide the myocardial–smooth muscle interface at the arterial pole (Waldo et al., 2005a). The SHF-derived myocardium gives rise to the conotruncal myocardium and development of this myocardium is critical for normal alignment of the two outflow vessels with respect to the ventricles (Yelbuz et al., 2002; Ward et al., 2005). Clinically, malalignment of the arterial pole occurs in the conotruncal defects, as seen in double outlet right ventricle (DORV) and tetralogy of Fallot. In both of these defects, the aorta overrides the ventricular septum. Recently, we have shown that CNC are needed for normal development of the myocardial component of the SHF prior to the time they begin septation of the outflow vessels (Waldo et al., 2005b). Ablation of the pre-migratory CNC results in both the absence of septation, as well as, malalignment of the arterial pole because of the failure of the SHF myocardium to develop normally. It is not known how CNC affect SHF development because the two cell populations are not in proximity when defective development of the SHF occurs.

In chick embryos, the CNC begin their migration into the caudal pharynx (arches 3–6) at stage 10 (Hamburger–Hamilton stages). At stage 12, the CNC pause in the circumpharyngeal

* Corresponding author. Fax: +1 919 668 1599.
E-mail address: mhutson@duke.edu (M.R. Hutson).
[1] Current address: Division of Gastroenterology, Department of Medicine, Duke University Medical Center, Durham, NC 27710, USA.
[2] Current address: Division of Cardiology, Department of Medicine, Duke University Medical Center, Durham, NC 27710, USA.

0012-1606/$ - see front matter © 2006 Elsevier Inc. All rights reserved.
doi:10.1016/j.ydbio.2006.02.052

ridge (Le Douarin et al., 1992; Kuratani and Kirby, 1992), and beginning at late stage 13, they populate the dorsal third pharyngeal arch by migrating between the pharyngeal ectoderm and endoderm. This is repeated as the succeeding arches 4 and 6 develop. It is during this period that the myocardium is added to the outflow tract from the SHF. At stage 22, almost 4 days after leaving the dorsal neural tube, CNC finally migrate into the cardiac outflow tract where they will form the aorticopulmonary septation complex that will divide the outflow into the aorta and pulmonary trunk.

The SHF is the splanchnic mesoderm located in the floor of the caudal pharynx behind the outflow attachment to the pharynx. Beginning at stage 14, the SHF migrates into the outflow providing truncal myocardium and allowing lengthening of the looping primary heart tube until stage 18 (Waldo et al., 2001, 2005a; Mjaatvedt et al., 2001; Kelly et al., 2001). Recently, we have shown that the heart tube is shortened and abnormally looped after neural crest ablation (NCA) because of the failure of the SHF-derived myocardium to migrate into the outflow and ultimately leads to malalignment of the outflow vessel (Yelbuz et al., 2002; Waldo et al., 2005b). Because abnormal looping occurs well before the CNC reach the outflow, the SHF-related defects appear to be caused indirectly by NCA (Hutson and Kirby, 2003). This suggests that CNC may modulate signaling factors in the pharynx.

The first evidence that fibroblast growth factor (FGF) 8 signaling was disrupted in the CNC-deficient pharynx came from a study examining the primary myocardial dysfunction also observed after NCA. We showed in culture that conditioned media from the NCA pharynx could reproduce the depressed myocardial Ca^{2+} transient of the primary heart tube and that the transient could be rescued with an FGF8b-neutralizing antibody (Farrell et al., 2001). This suggested that FGF signaling was elevated after NCA.

FGF8 provides a variety of mitogenic, survival, pro- or anti-differentiation signals to pattern tissues and is required for normal craniofacial, cardiac and limb development (Schneider et al., 2001; Alsan and Schultheiss, 2002; Crossley and Martin, 1995; Crossley et al., 1996). Although there are at least 4 to 8 alternatively spliced *FGF8* isoforms in humans and mouse, the chick only produces 2 isoforms: *fgf8a* and *fgf8b* (Basilico and Moscatelli, 1992; Haworth et al., 2005). FGF8b isoform has been shown in the literature to be more biologically potent than FGF8a isoform. Most of the in vivo embryological studies comparing the biological activity of the isoforms have been done by the Nakamura and colleagues working in the chick hindbrain. They have shown that FGF8b isoform is 100 times more potent than FGF8a (Sato et al., 2001). The FGF8a and FGF8b isoforms differ by only 11 amino acids. A recent publication elucidating the crystal structure of FGF8b, FGF8a and the FGF receptors has shown that these 11 amino acids greatly enhance the binding affinity of the FGF8b isoform to the FGF receptors whereas the FGF8a isoform has very low binding affinity and this accounts for the potent biological activity of the FGF8b isoform (Olsen et al., 2006). FGF signaling is mediated via tyrosine kinase receptors (FGFRs) that act through a number of transduction pathways. While FGF8-null mice die during gastrulation (Meyers et al., 1998; Sun et al., 1999; Moon and Capecchi, 2000), hypomorphic mice have cardiac outflow, pharyngeal arch artery and pharyngeal gland defects reminiscent of the NCA phenotype (Abu-Issa et al., 2002; Frank et al., 2002).

Fgf8 is expressed in the lateral pharyngeal ectoderm and endoderm at the time CNC begin to populate the caudal pharyngeal arches and as the myocardium is added to the looping heart from the SHF (Farrell et al., 2001). Because FGF8b antibody rescued the myocardial calcium transient in culture, we hypothesized that FGF8 signaling is overabundant in the pharynx in the absence of the CNC. This excessive signaling prevents addition of myocardium from the SHF causing a shortened outflow tract that ultimately results in cardiac arterial pole alignment defects.

In this study, we demonstrate by quantitative PCR that total *fgf8* and *fgf8b* message and downstream targets are elevated in the caudal pharynx in NCA embryos between stages12 and 14, coinciding with the time the CNC should enter the pharynx. Using an FGF reporter in transiently transfected cells, we determined that the FGF8b isoform has much more potent signaling properties than FGF8a. Also using this reporter, we were able to show that FGF8 signaling was increased in the pharynx after NCA. All of the indirect effects of NCA, i.e. looping, addition of myocardium from the SHF, myocardial function and arterial pole alignment, could be rescued in ovo by treating the embryos with either anti-FGF8b or the FGFR blocker, SU5402. This rescue was time and dose-dependent. Conversely, reducing FGF8 signaling below normal levels in sham-operated embryos resulted in failure of myocardial addition from the SHF, abnormal looping and arterial pole alignment defects.

Materials and methods

Embryo preparation

NCA and sham-operated embryos were prepared as described previously (Waldo et al., 1996). At Hamburger and Hamilton stage 10, the vitelline membrane was torn. FGF8b function blocking antibody (varying concentrations between 40 and 400 μM, R&D Systems), 10–20 μM of the FGFR1 blocking compound SU5402 (Calbiochem, La Jolla, CA), PBS (control for FGF8b antibody) or DMSO/PBS (1:1000 in PBS, SU5402 control) was dropped onto the embryos. The embryos were incubated for 24 h (stages 14–16), assessed for heart looping and collected for either immunohistochemistry or myocardial calcium transient measurements (see below). Some embryos were incubated until day 9 and examined histologically for arterial pole alignment. In a second series of experiments, embryos were treated with the anti-FGF8b 24 h after NCA and assessed for arterial pole alignment at day 9. In all experiments, no differences were observed between PBS and DMSO/PBS treated control embryos, and therefore are reported as PBS controls. For cell tracing experiments, SHFs were injected at stage 14 with Tetramethylrhodamine-succinyl ester (TAMRA-SE, Molecular Probes) as previously described (Ward et al., 2005) and examined for migration into the outflow at stage 18.

Quantitative RT-PCR

RNA was isolated from caudal pharynges of sham or NCA embryos between stages 12- and 15 using RNAeasy minicolumn (Qiagen) and reverse transcribed using SuperScript II reverse transcriptase (Invitrogen). A minimum of 11 pools of RNA was isolated for each stage and condition. Real-time quantitative PCR analysis was performed with primers specific for *hprt*, and *18S*, *fgf8t*, *fgf8b*, as well as the FGF8 downstream target genes, *Pea3*, *Erm*, *Er81* and *mkp3* using IcQ Supermix containing SYBR Green (Bio-Rad) with a Bio-Rad quantitative

real-time iCycler. See Supplementary data for primer sequences. All reactions were normalized to *hprt* and *18S* standards. Fold change in expression was determined by setting sham expression levels at one and plotting the relative expression levels of each gene at each stage in the NCA caudal pharynx. Significant differences were calculated by unpaired Student's *t* test with unequal variance.

Tissue culture and transfections

To find conserved elements within the *mkp3* promoter, we compared 100 kb of DNA sequence upstream of the human, mouse, rat, dog, chicken, frog and zebrafish *mkp3* genes, using the BLAST program. Four conserved regions were identified spanning about 3000 bp proximal to the 5′UTR that shared over 75% homology. A 1.9 kb fragment (see Supplementary methods for primer sequences) was cloned into the GFP expression vector, pEGFPN-1. COS7 cells were used for all the transient transfection experiments. The cells were cultured in DMEM and 10% fetal bovine serum (Gibco) until 80% confluent. Next, COS7 cells were transiently transfected with the *mkp3*-GFP expression vector using FuGene (Roche) following the manufactures protocols. Transfected COS7 cells were split to multiwell plates and exposed for 6 h to varying concentrations of FGF8b, VEGF or EGF proteins, alone or in combination with the respective antibodies (R&D Systems) in serum-free media in duplicate. Conditioned media was generated from caudal pharynx explants cultured overnight in serum-free media. For the caudal pharynx explant co-culture or conditioned media experiments, transfected cells were cultured overnight alone or in combination with 100 μM anti-FGF8b (R&D Systems) in serum free media. To test the difference in FGF8a versus FGF8b signaling, FGF8a or FGF8b expression vectors (kind gift of Dr. H. Nakamura, Tohoku University, Japan) were transfected into COS7 cells. Serum-free conditioned media from these cells were collected and placed on *mkp3*-GFP transfected COS7 cells with or without anti-FGF8b in duplicate. All responses were measured by photographing 5 fields of cells at a set exposure (to avoid counting cells with very low GFP expression) and counting the number of GFP expressing cells compared to total number of cells stained with the Hoechst (Molecular Probes) nuclear marker following the manufacturer's protocol for staining in live cells. Each measurement represents an average of a minimum of 2 duplicates in at least 3 separate experiments. Statistical analysis for Mkp3-GFP reporter experiments was unpaired Student's *t* test with unequal variance.

Myocardial calcium transient measurement

Heart tubes minus the presumptive atria were dissected from stage 14–16 embryos and loaded with the fluorescent Ca^{2+} indicators, fura-2 or fluo-4, using the AM ester forms. Ca^{2+} transients were recorded in the ventricular region of spontaneously beating hearts at 100 Hz sampling rate with a microspectrofluorometer DeltaScan system from Photon Technology International as previously described for Ca^{2+} measurements in explant cultures of cardiac muscle strips (Farrell et al., 2001). For fluo-4, Ca^{2+} concentration was calculated from:

$$[Ca^{2+}]_i = K_D R/((K_D/[Ca^{2+}]_{rest}) - R + 1)$$

where the K_D = 1000 nM (Molecular Probes Handbook), R is the number of photon counts and $[Ca^{2+}]_{rest}$ is the resting Ca^{2+} set at 250 nM (Creazzo et al., 2004). Measurements were carried out without knowledge of the embryo treatment.

Immunohistochemistry and cell proliferation

Sham, NCA and NCA embryos treated with or without anti-FGF8b or SU5402 were collected at stage 15, fixed with Methacarn, embedded in paraffin and sectioned for immunostaining. HNK-1 (ATCC), visualized with Alexa 488 goat anti-mouse secondary antibody (Molecular Probes) and MF20 (Developmental Studies Hybridoma Bank developed by NICHD and maintained by the University of Iowa, Department of Biological Sciences) visualized with Alexa 568 goat anti-mouse secondary antibody were carried out as previously described (Waldo et al., 1996, 1998). BrdU incorporation visualized with Alexa488 goat anti-mouse secondary antibody was detected as previously described (Waldo et al., 2005b). The nuclei were stained with Hoechst (Molecular Probes) following the manufacturer's protocol. The number of BrdU-positive cells was counted in populations of 50 cells in sagittal sections. Ten sections for a total of 500 cells were counted per embryo (n = 3 embryos for each treatment). Statistical analysis used was Student's *t* test.

Assessment of arterial pole alignment

Hearts from sham-operated and NCA embryos treated with PBS, anti-FGF8b or SU5402 at stage 10 were harvested at day 9 and arterial pole alignment was documented. The hearts were fixed overnight in 10% formalin, paraffin embedded, serially sectioned and stained with hematoxylin and eosin. The arterial pole was scored as malaligned if the aorta or the aortic portion of the outflow was not wedged between the tricuspid and mitral valve and shifted to the right in relation to the pulmonary trunk.

Results

FGF8 signaling is increased after cardiac neural crest ablation

To determine if FGF8 signaling is increased in the caudal pharynx after NCA, we designed specific primers to total *fgf8* (*fgf8t*), *fgf8b* and several known downstream targets of FGF8 signaling including the dual phosphatase, *mkp3* and the transcription factors, *pea3*, *erm* and *er81* for quantitative PCR (Fig. 1A). Beginning at stage 12, 24 h after NCA, when CNC are normally located in the circumpharyngeal ridge, *fgf8t* and *fgf8b* messages were significantly, albeit slightly, increased in the caudal pharynx from NCA embryos when compared to sham-operated embryos. At this stage, there was no difference in the expression levels of FGF8 downstream target genes (Fig. 1A). Interestingly, the increase in *fgf8b* expression accounted for the increase in *fgf8t*. By stage 13, there was almost a 3-fold increase in expression of *fgf8t* and *fgf8b* in the NCA caudal pharynx. This accompanied a significant increase in *mkp3* expression. *Mkp3* has been previously reported to be one of the earliest downstream targets to respond to FGF8 signaling (Kawakami et al., 2003). At stage 14, when the myocardium from the SHF normally begins to migrate into and lengthen the cardiac outflow, *fgf8b* expression was still significantly increased in the NCA pharynx. *Mkp3* remained elevated, and now *pea3* and *erm* were significantly increased. By stage 15, *fgf8t* and *fgf8b* message levels in the NCA pharynx were not different from sham, but all of the FGF8 target genes tested were significantly increased. This suggests that the quantity of FGF8 signaling is increased in the NCA caudal pharynx at a critical time for the migration of the myocardium from the SHF into the outflow tract.

To determine whether the increases in message for *fgf8* and FGF8 downstream targets represent an increase in FGF8 signaling, we designed an expression plasmid that would report FGF8 signaling. *Mkp3* has been used previously as an FGF8 reporter (Kawakami et al., 2003). A reporter construct comprising 1.9 kb upstream regulatory sequence of chick *mkp3* fused to GFP was transfected into COS7 cells. The cells were exposed to increasing concentrations of FGF8b protein. A linear GFP response was elicited by 1.0–10 ng of FGF8b (Fig. 1B). The FGF8b activation of *mkp3*-GFP could be completely inhibited by the function blocking FGF8b antibody (Fig. 1B) or the

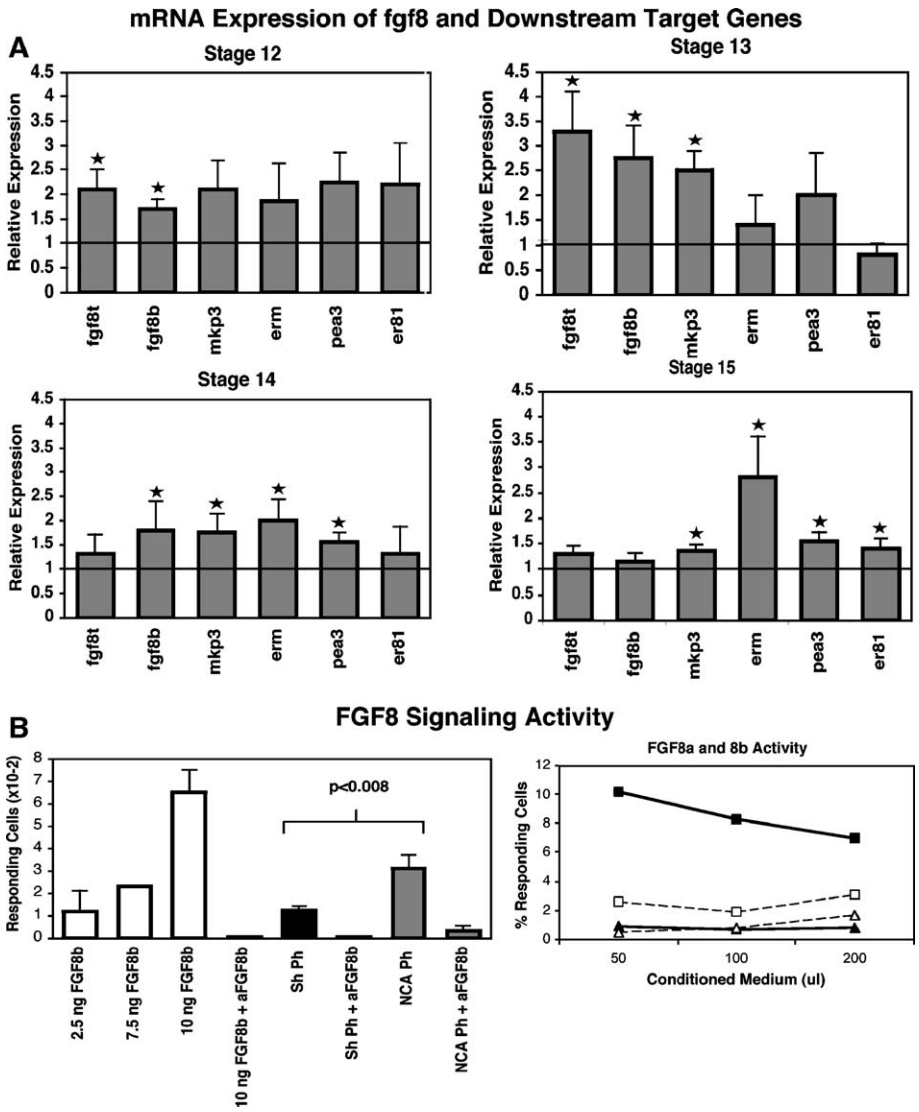

Fig. 1. FGF signaling is increased after NCA. (A) Quantitative PCR analysis of *fgf8t*, *fgf8b*, *mkp3*, *erm*, *pea3* and *er81* in caudal pharynx from stages 12–15 NCA embryos. Expression in NCA pharynx (grey bars) is plotted relative to the sham levels set at one (black line). Stars indicate significance. Bars equal SEM. *fgf8t* and *fgf8b* are increased in NCA pharynx at stage 12 ($n = 11$, $P < 0.05$) and stage 13 ($n = 11$, $P < 0.04$). At stage 13, *mkp3* ($P < 0.05$) expression in NCA pharynx is significantly increased compared to sham. At stage 14 ($n = 13$), expression of *fgf8b* ($P < 0.03$) and all but one of the downstream target genes are significantly increased (*pea3* $P < 0.02$; *erm* and *mkp3* $P < 0.05$) in the pharynx after NCA. By stage 15 ($n = 15$), only the downstream targets are significantly elevated (*erm* and *pea3* $P < 0.01$; *er81* $P < 0.04$; *mkp3* $P < 0.02$). (B) COS7 cells transiently transfected with *mkp3*-GFP respond to FGF signaling. *Mkp3*-GFP is activated by increasing concentrations of FGF8b (white bar). Maximal response is reached with 10 ng FGF8b. More *mkp3*-GFP is activated in the cells co-cultured with NCA pharynx (NCA Ph, $n = 5$) compared to the sham pharynx (Sh Ph, $n = 5$, $P < 0.008$). Anti-FGF8b (aFGF8b) inhibits activation. (C) FGF8b isoform is more active than FGF8a isoform. *Mkp3*-GFP reporter cells cultured with increasing volumes of conditioned media from either FGF8a or FGF8b expressing cells. FGF8b conditioned media produce maximal *Mkp3*-GFP response (black squares) that is inhibited by anti-FGF8b (open squares). FGF8a (black triangles) or FGF8a plus anti-FGF8b (open triangles) exhibits very low *Mkp3*-GFP activity. Error bars equal SD.

chemical FGFR1 inhibitor, SU5402 (data not shown). VEGF, EGF and retinoic acid did not elicit a response from the reporter (see supplemental data).

To compare the signaling capacity of chick FGF8a versus FGF8b, we transiently transfected plasmids expressing either FGF8a or FGF8b into a second set of COS cells. After 24 h, 50–200 μl of the supernatant from these cells was placed on COS cells transiently transfected with the *mkp3*-GFP reporter construct. There was a maximal response of the reporter cells to increasing amounts of supernatant from the cells expressing FGF8b (black box line Fig. 1C). The response could be blocked by anti-FGF8b (open box line Fig. 1C). There was no response to the supernatant from cells expressing FGF8a (black triangle line in Fig. 1C). These results confirm the results of Sato et al. (2001) who used in vivo electroporations to show that the effectiveness of FGF8a is 100-fold less than that of FGF8b in patterning the mid-hindbrain region.

After establishing the response characteristics of the reporter construct to FGF8 signaling, we co-cultured COS7 cells transiently transfected with the *mkp3*-GFP reporter with explants of dissected caudal pharynx from stage 14 (when most of the downstream targets are elevated) sham-operated or NCA

embryos. The *mkp3*-GFP reporter cells showed significantly more FGF8 signaling in the caudal pharynx from NCA embryos as compared with the shams. The response to both tissues was specifically inhibited by anti-FGF8b (Fig. 1B). These data show that there is elevated FGF8b signaling in the caudal pharynx in the absence of CNC at a time critical for the migration and differentiation of the myocardial component of the SHF.

Reducing FGF signaling rescues the early indirect affects of cardiac neural crest ablation

Because excess FGF8 signaling in the caudal pharynx coincided with the time when the myocardial component of the SHF is added to the outflow tract, we attempted to rescue looping and addition of myocardium from the SHF by reducing the level of FGF8 signaling after NCA. Normally in stage 15 embryos, the inflow limb of the heart loop partially obscures the outflow limb when viewed from the left (Fig. 2A). After NCA, the outflow limb is displaced ventrally and cranially, so that both the outflow and inflow limbs are visible when viewed from the left (Fig. 2B). This abnormal looping is due to a failure of the SHF to add myocardium that normally lengthens the outflow portion of the heart tube (Yelbuz et al., 2002; Waldo et al., 2005b), and is one of the first defects observed after NCA. We examined looping in the NCA embryos treated with FGF8 antibody or SU5402 to determine if heart looping could be rescued. Looping was normal in 67% and 50% of the NCA embryos treated with antibody or SU5402 as compared to only 23% of untreated NCA embryos (Table 1, Figs. 2D, F and G). Interestingly, looping was abnormal in sham-operated embryos treated with either the FGF8b antibody or SU5402 (Figs. 2C and E). Only 33% (SU5402) and 53% (anti-FGF8b) showed normal looping (Table 1). This suggests that normal cardiac looping is sensitive to FGF8 signaling. Evidence that FGF8 signaling was specifically inhibited in these embryos is corroborated by abnormal forebrain and frontonasal development in the shams treated with FGF8 inhibitors (Figs. 2C and E). The frontonasal region has been shown to require FGF8 signaling for normal development.

Previously, we have shown that cells migrating from the SHF express HNK-1 as they move into the outflow tract and differentiate into myocardium (Waldo et al., 2001, 2005a). After NCA, HNK-1 expression is significantly reduced during the myocardial migratory phase in the SHF, indicating that the myocardial cells derived from the SHF are not incorporated into the outflow myocardium after NCA (Figs. 3A and B) (Yelbuz et al., 2002; Waldo et al., 2005b). We examined HNK-1 expression in NCA embryos 24 h after treatment with either anti-FGF8b or SU5402 to see if the myocardial migration from the SHF migration could be rescued. Both SU5402 and the FGF8b antibody rescued HNK-1 expression in the SHF (arrows in Figs. 3C and D).

To directly show that the migration of the SHF cells was rescued in the NCA embryos treated with anti-FGF8b, we labeled the SHF with DiI and caged rhodamine, and examined the embryos 24 h later for labeled cells in the outflow myocardium. Labeled myocardial cells were found in the outflow

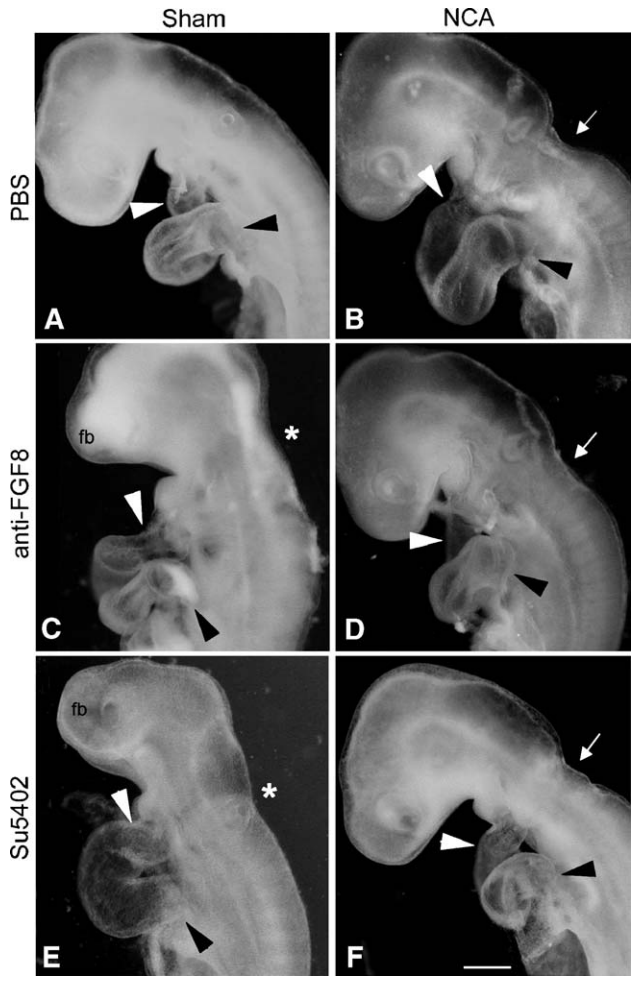

Fig. 2. FGF8b antibody (anti-FGF8b) or SU5402 treatment normalizes heart looping 24 h after NCA. (A) Normal heart loop viewed from the left of stage 15 sham-operated embryo treated with PBS shows the outflow portion of the loop (white arrowhead) partially obscured by the inflow portion of the loop (black arrowhead). (B) Abnormal heart loop in PBS-treated NCA embryo shows outflow portion of the loop (white arrowhead) and the inflow portion (black arrowhead) are completely visible. (C) Sham-operated embryo after anti-FGF8 treatment has abnormal heart looping. Note the blunted forebrain (fb). (D) Heart looping appears normal in an NCA embryo after anti-FGF8 treatment. (E) Heart tube in sham embryo is abnormally looped after SU5402 treatment. (F) Normally looped heart tube in an SU5402-treated NCA embryo. White arrows mark the hindbrain defect caused by the NCA in panels B, D, and F. Asterisk marks flattened hindbrain in shams treated with anti-FGF8 and SU5402. Scale bar = 0.15 mm.

tract of sham embryos treated with PBS and in the neural crest-ablated embryos treated with anti-FGF8b (Figs. 3E and H), while as previously described, none were found in the NCA embryo (Waldo et al., 2005b and Fig. 3F). The embryos were sectioned to confirm that the labeling was in the myocardial layer (data not shown). Rescue of the myocardial component by reducing FGF8 signaling in NCA embryos suggests that the SHF is exposed to too much FGF8 signaling when CNC are not present in the caudal pharynx. Interestingly, the sham-operated embryos treated with anti-FGF8b had no labeled myocardial cells in the outflow (Fig. 3G). Therefore, the abnormally looped and shortened outflow tract observed in sham-operated embryos in which FGF8 signaling is reduced to below normal levels is

Table 1
Summary of heart looping phenotype in all treatment groups

Treatment	% normal heart looping
Sham + PBS (n = 11)	90
NCA + PBS (n = 13)	23
NCA + anti-FGF8 (n = 18)	67
NCA + SU 5402 (n = 8)	50
Sham + anti-FGF8 (n = 15)	53
Sham + SU 5402 (n = 6)	33

likely due to the failure of the SHF-derived outflow myocardium to migrate into the heart tube. Hence, the migration of SHF-derived myocardium is particularly sensitive to FGF8 levels.

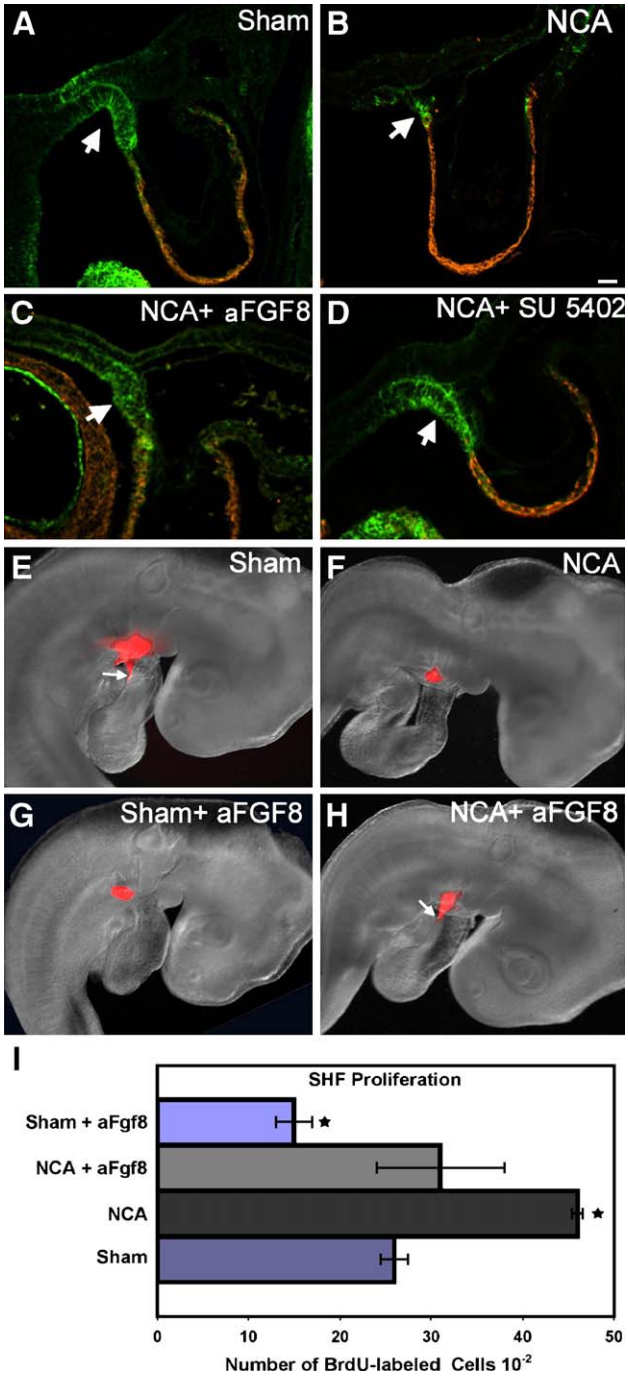

Recently, we have shown that there is an increase in proliferation in the SHF in NCA embryos (Waldo et al., 2005b). If FGF8 oversignaling is causing increased proliferation, we would predict that treatment with FGF8b antibody would reduce proliferation to normal levels. We examined BrdU incorporation in sham and NCA stage 15 embryos with or without anti-FGF8b treatment. Sham embryos treated with PBS had an average of 26% BrdU-positive cells as compared with 46% after NCA ($P < 0.0001$, Fig. 3I and Supplementary Fig. 2). Proliferation was decreased to 31% BrdU-positive cells in NCA embryos treated with anti-FGF8b, which was not significantly different from the number of proliferating cells in sham embryos ($P = 0.15$), but was significantly lower when compared to the untreated NCA group ($P = 0.01$, Fig. 3I, and Supplementary Fig. 2). This indicates that the anti-FGF8b treatment normalizes proliferation in the SHF of NCA embryos. Interestingly, proliferation in sham-operated embryos treated with anti-FGF8b was significantly lower: 15% of the cells were BrdU positive, a dramatic reduction when compared to the sham or neural crest-ablated embryos not treated with anti-FGF8b or NCA embryos treated with anti-FGF8b ($P < 0.0001$). These data suggest that proliferation and migration of the myocardial component of the SHF are linked to precisely controlled levels of FGF8 signaling.

Previously we have shown that the myocardial calcium transient is depressed more than 30% in stage 14 chick embryos after NCA (Waldo et al., 1999). To test if the Ca^{2+} transient could be rescued, we treated NCA embryos in ovo with either FGF8b antibody or SU5402 within 4 h after the ablation (stages 9–10). At stage 14, the presumptive ventricular regions of the heart tubes were excised for myocardial Ca^{2+} transient measurements. Fig. 4 shows that the magnitude of the myocardial Ca^{2+} transient was reduced after NCA when compared to the sham-operated control. Treatment with either FGF8b antibody or SU5402 restored the myocardial Ca^{2+} transient to its normal level in NCA embryos. With either treatment, the magnitudes of the transients were generally larger than those in the sham controls (Figs. 4A–C). There were no apparent differences in the diastolic Ca^{2+} level, consistent with previous observations (Creazzo et al., 1997; Farrell et al., 2001).

Fig. 3. FGF8 antibody or SU5402 rescues migration and proliferation of the SHF in neural crest-ablated embryos. Sagittal sections through the outflow and SHF (white arrow A–D) of a stage 16 chick, stained for HNK-1 (green, migrating SHF) and MF-20 (red, myocardium). (A) The SHF expresses HNK-1 as it migrates into the caudal outflow. (B) The SHF in the NCA embryo expresses very little HNK-1. HNK-1 expression is restored to normal in an NCA embryo 24 h after treatment with anti-FGF8 (C) or SU5402 (D). (E–H) Stage 18 chick embryos 24 h after labeling SHF with DiI and caged rhodamine. SHF cells migrate into the outflow (white arrows) in the sham (E) and the NCA treated with anti-FGF8 (H). No labeled myocardial cells are found in the NCA (F) or sham-operated embryos treated with anti-FGF8 (G). (I) Graph showing average number of BrdU positive cells per 100 cells counted in the SHF. The SHF of NCA embryos showed a significant increase in the number of BrdU-positive cells (star) as compared to shams. Proliferation in SHF from NCA treated with anti-FGF8b was not significantly different from sham ($P = 0.15$). Proliferation in shams treated with aFGF8 is significantly lower than PBS treated shams ($P = 0.0007$). Error bars represent SD. Scale bar = 50 um for A–D.

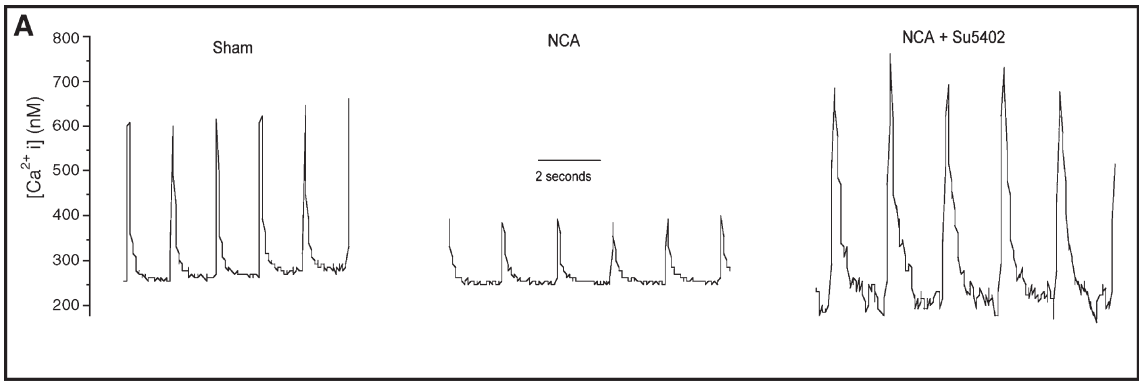

B

Treatment	% Change in Ca^{2+} over baseline
Sham + PBS (n=8)	93%
NCA+ PBS (n=11)	50%
NCA + anti-FGF8 (n=8)	132%

C

Treatment	% Change in Ca^{2+} over baseline
Sham +DMSO/PBS (n=6)	105%
NCA+ DMSO/PBS (n=11)	58%
NCA + SU 5402 (n=7)	142%

Fig. 4. Anti-FGF8b or SU5402 treatment rescues Ca^{2+} transients after NCA. (A) An example of Ca^{2+} transients in the ventricular region of stage 14 hearts in sham-operated controls, after NCA alone or NCA with treatment of the embryo with SU5402. The Ca^{2+} transient that is reduced after NCA is restored to normal when treated with SU5402. (B and C) Average percent increase in the magnitude of the Ca^{2+} transient in anti-FGF8 (B) or SU5402 (C) treatments. Both treatments restored the Ca^{2+} transient to normal after NCA. Single factor ANOVA indicated significance at $P = 0.02$ and $P = 0.003$ for anti-FGF8 antibody and SU5402 treatment, respectively.

Taken together, these results indicate that all of the early effects of NCA, i.e. abnormal looping, addition of myocardium from the SHF to the outflow tract, proliferation of cells in the SHF and myocardial calcium transient, are rescued by treatment of the embryos with FGF8 blocking agents.

Inhibition of FGF8 signaling rescues arterial pole alignment in NCA embryos

The final position of the arterial pole is attained during the later stages of outflow septation when the aortic side of the outflow tract nestles or "wedges" between the atrioventricular valves (Figs. 5A–A″). In chick, outflow septation and alignment are complete by embryonic day 8. Malalignment of the arterial pole occurs when the aortic side of the outflow fails to wedge between the atrioventricular valves and stays in a "side-by-side" orientation with the pulmonary artery. In NCA embryos, not only does the aorticopulmonary septum fail to form, but the common outflow vessel is shifted to the right to arise from the right ventricle (Figs. 5B–B″). Even though separate aortic and pulmonary arterial trunks do not form, the aortic and pulmonary sides of the common arterial trunk can be identified by the positions of the coronary artery ostia. Thus, Fig. 5B″ shows the side-by-side relationship of the aortic and pulmonary components of the common trunk (compare with Fig. 5A″).

Because the early defects could be rescued by reducing FGF signaling, we wondered if the final outflow alignment could also be rescued. NCA embryos were treated with anti-FGF8b or SU5402 at stage 9–10 and re-incubated until embryonic day 9 when the hearts were analyzed for outflow alignment. All hearts from untreated NCA embryos had PTA (Table 2). The majority of these common trunks (88%) failed to wedge with respect to the inflow valves and were shifted to the right (compare Figs. 5A″ with Fig. 5B″). Because the CNC that make the aorticopulmonary septum are missing, the anti-FGF8b or SU5402 treatment was not expected to rescue the PTA. However, wedging of the aortic side of the common outflow was rescued in 78% and 100%, respectively, of the NCA embryos treated with anti-FGF8 ($n = 7$, Figs. 5C–C″) or SU5402 ($n = 6$, Figs. 5D–D″). In addition, the ventricular septal defect in all of the rescued hearts was smaller and closer to the outflow valves, when compared to the untreated NCA hearts (arrowhead in Figs. 5B, C′ and D′).

Decreasing FGF8 signaling in sham embryos causes arterial pole defects

Because decreasing FGF8 signaling in sham-operated embryos caused abnormal development of the SHF, we examined hearts from shams treated with either anti-FGF8 or SU5402 to determine if the aorta and pulmonary trunk were malaligned. An overriding aorta in a side-by-side orientation with the pulmonary trunk occurred in 42% and 54%, respectively of anti-FGF8b- or SU5402-treated embryos (Table 2, Figs. 6C–D). Pulmonary stenosis or atresia, a hallmark of tetralogy of Fallot, was observed in 2 hearts (Figs. 6E–F). Normally by this stage in heart development, the left 4th arch artery has disappeared (Fig. 6A) but in the heart shown in Fig. 6E there was a persisting left 4th arch artery. The most severe defect was seen in one heart with transposition of the great arteries (Figs. 6G–H) with a common atrioventricular canal (data not shown). The left

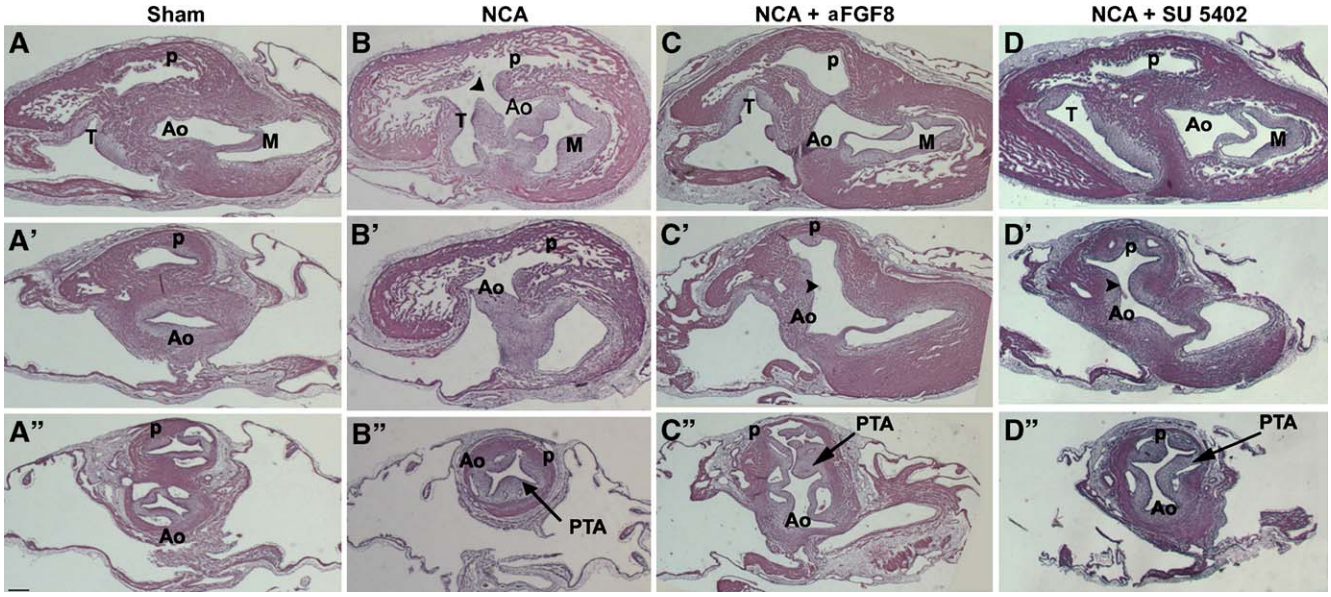

Fig. 5. FGF8 antibody or SU5402 treatment restores wedging of the aortic side of the outflow in day 9 hearts of NCA embryos. Hematoxylin and eosin stained transverse sections of hearts beginning at the level of the inflow valves and progressing distally to the level of the outflow valves. (A–A″) Sham-operated embryo treated with PBS shows that the aortic outlet (Ao) is wedged between the tricuspid (T) and mitral (M) valves. The aortic outlet stays in this position in the more distal sections at the level of the semilunar valves (A′ and A″). (B–B″) PBS-treated NCA embryo has a ventricular septal defect (black arrowhead in panel B) at the level of the tricuspid and mitral valves with the aortic outlet shifted to the right. The aortic portion of the PTA is not wedged and stays to the right of the pulmonary portion of the outflow even at the level of the semilunar valves (B″) indicating the aortic side of the outflow is malaligned over the right ventricle (compare A″ with B″). Anti-FGF8-treated NCA (C–C″) and SU5402-treated NCA (D–D″) embryos have a ventricular septal defect (black arrowhead panels C′ and D′) in a more distal position compared to the NCA plus PBS (compare with panel B). With either treatment, the aortic outlet is wedged between the tricuspid and mitral valves and remains wedged behind the pulmonary portion of the common outflow (C″ and D″) indicating a rescue of arterial pole alignment even though PTA still occurs (compare panels A″, B″, C″ and D″). Scale bar = 100 μm.

ventricular outlet was wedged between the atrioventricular valves but divided into the right and left ductus arteriosus indicating that it was the pulmonary trunk rather than the aorta. The right ventricular outlet was in the normal position but ultimately divided into the systemic arteries including the persisting left 4th arch artery (Figs. 6H–H′). Therefore, the aorta originated entirely from the right ventricle and the pulmonary trunk originated from the left ventricle. These results suggest that addition of the myocardial cells from the SHF to the outflow tract is critical for normal looping which is necessary for normal arterial pole alignment.

Time and amount of reduction in FGF8 signaling are important for alignment

The rescue of arterial pole alignment was dose- and time-dependent. None of the hearts from NCA embryos treated with greater than 100 μM of the anti-FGF8 had wedging of the aortic side of the common trunk (data not shown, Table 2, $n = 7$). These data taken together with the arterial pole malalignments in the sham-treated group suggest that too much or too little FGF8 signaling is detrimental for arterial pole development and viability.

Interestingly, when the sham-operated embryos were treated with a lower dose of FGF8 antibody (40 μM), arterial pole alignment and septation were normal but the neural crest-derived smooth muscle tunics of the great arteries were much thicker than normal (4 out of 4 embryos, Figs. 6I and J). The walls were so overgrown that the lumens of the vessels were almost completely occluded. This thickening was not observed with the higher doses of anti-FGF8 antibody. These results suggest that the arterial pole and the arch arteries require different levels of FGF signaling for normal development.

Table 2
Summary of arterial pole alignment defects at day 9

Treatment	Concentration	Wedged	PTA	Ov Ao	Pul Sten	Ao Ar Sten	Total
NCA + PBS	1×	2 (12%)	16	14 (88%)			16
NCA + anti-FGF	40 μM–100 μM	7 (78%)	9	2 (22%)	1		9
NCA + anti-FGF	>100 μM	0	7	7 (100%)			7
NCA + SU 5402	20 μM	6 (100%)	5	0			6
Sham + PBS	1×	12 (100%)	0	0			12
Sham + anti-FGF	40 μM	3 (75%)	0	1 (25%)		4	4
Sham + anti-FGF	100 μM	15 (58%)	0	11 (42%)	1		26
Sham + SU 5402	20 μM	6 (46%)	0	7 (54%)	1		13

Abbreviations: PTA, persistent truncus arteriosus; Ov Ao, overriding aorta; Pul sten, pulmonary stenosis; Ao Ar Sten, aortic arch artery stenosis.

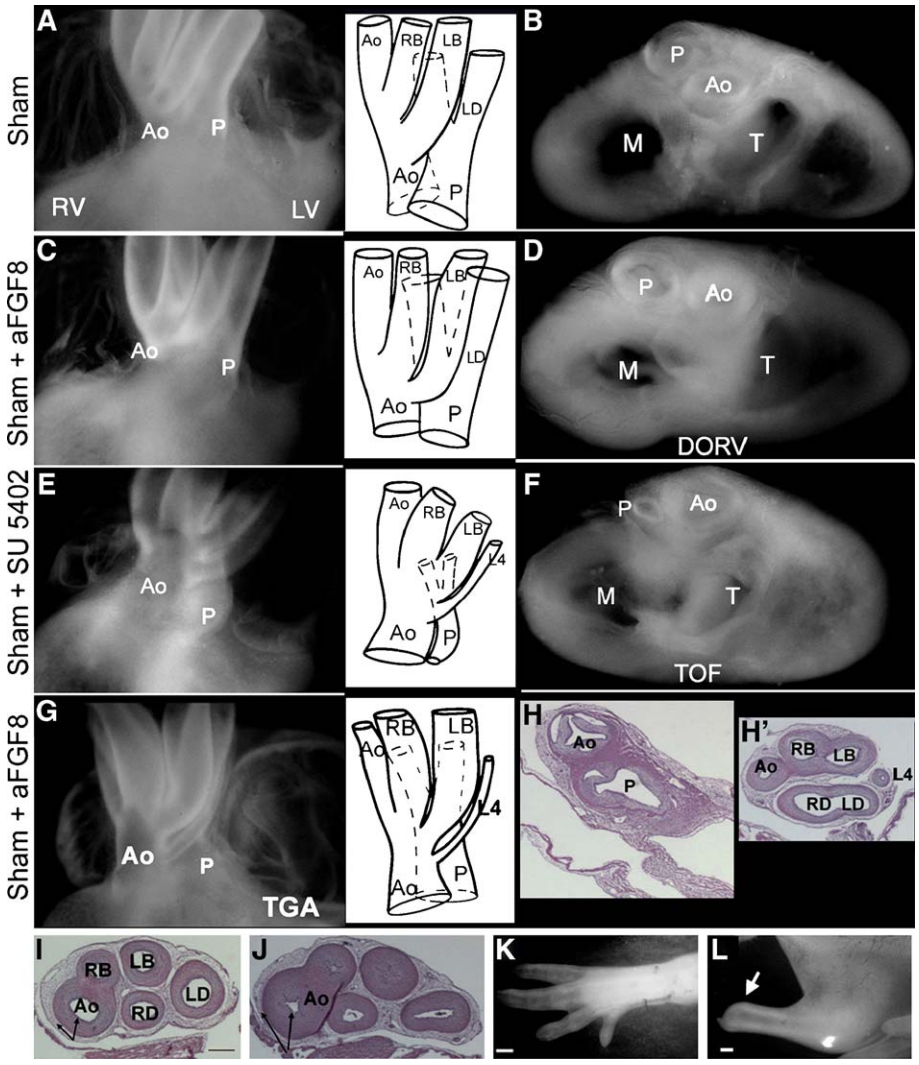

Fig. 6. Reducing normal levels of FGF signaling causes arterial pole alignment defects. (A, C, E and G) Ventral view of whole hearts and line drawings shows the position of outflow vessels and arch artery derivatives in day 9 hearts. (B, D and F) Atria have been dissected away to show a 4-valve view. (A) Sham PBS-treated heart has normal wedging and alignment of the aorta (Ao) behind the pulmonary (P) and between the mitral and tricuspid valves (M and T in B). (C and D) Anti-FGF8-treated sham with DORV has the characteristic side-by-side position of the aorta and pulmonary trunk. (E and F). Pulmonary atresia in SU5402-treated sham with the aorta displaced to the right comparable to Tetralogy of Fallot (TOF). (G, H and H′) Anti-FGF8-treated sham shows the aorta ventral to the pulmonary trunk, similar to transposition of the great arteries (TGA). (H and H′) Sections indicate transposed aorta and pulmonary trunk. The pulmonary, dividing into right and left ductus arteriosus (RD and LD), arises from the left ventricular outlet while the aorta, dividing into the right and left brachiocephalics (RB and LB), arises from the right ventricular outlet. (I and J) The smooth muscle wall (arrows) of the aortic arch arteries in a sham embryo treated with 40 μM of anti-FGF8 (J) is thickened compared to the sham (I). (L) Truncated lower limb of NCA embryo treated with anti-FGF8 at stage 14 (compare to PBS-treated K). L4, left 4th arch artery (Black scale bar = 100 μm; white scale bar = 1 mm).

Timing of FGF8 inhibition was also a factor in whether or not the treatment affected arterial pole alignment. When NCA embryos were treated with anti-FGF8 or SU5402 at stage 14, a time when the SHF has already begun to lengthen the outflow, alignment of the arterial pole was not rescued. None of the hearts showed wedging of the aortic side of the common trunk ($n = 5$, data not shown). In addition, none of the sham-operated embryos treated at stage 14 with antibody had arterial pole malalignment defects. However, the efficacy of the antibody could be seen in limb truncations that occurred in both sham and NCA groups (Figs. 6K and L). No limb defects were observed in the embryos treated at earlier times. The limb defects were expected as FGF8 signaling has been shown by many groups to be required for limb outgrowth (Mahmood et al., 1995; Martin, 2001). The lack of limb defects in the earlier treatment group suggests that FGF8 antibody and SU5402 inhibit FGF signaling for a limited time.

Discussion

This study shows that the SHF is particularly sensitive to FGF8 because too much or too little FGF8 signaling results in abnormal development of the myocardial component of the SHF that leads to arterial pole alignment defects. Abnormal development of the myocardial component of the SHF is manifest as too much or too little proliferation of the myocardial

precursor cells in the SHF, which appears to be incompatible with normal migration and differentiation. Finally, we show that pulmonary stenosis is the result of defective development of the SHF and not defective outflow septation.

The SHF adds myocardium and later smooth muscle to the outflow end of the heart tube to form the myocardial-to-smooth muscle junction of the arterial pole at the level of the semilunar valves. In previous studies, we have shown that NCA results in abnormal heart tube looping, failure of the myocardial component of the SHF to migrate, decreased myocardial volume and increased in proliferation of the SHF cells. These are all defects indirectly caused by NCA (Yelbuz et al., 2002, 2003; Waldo et al., 2005b) because the defects are initiated a full 2 days before the CNC arrive in the distal outflow tract and because the CNC are not in physical proximity of the SHF at the time when abnormal development is first seen. The findings led us to the hypothesis that FGF8 signaling in the caudal pharynx is misregulated in the absence of cardiac neural crest.

The importance of FGF8 signaling in arterial pole development is supported by studies in mouse and human. In humans, DiGeorge and velocardiofacial syndromes are associated with the deletion of chromosome 22q11.2. TBX1, a T-box containing transcription factor expressed in the SHF, has been identified in mouse genetic models of 22q11.2 deletion (Jerome and Papaioannou, 2001; Lindsay et al., 1999, 2001; Merscher et al., 2001) and studies in human patients (Yagi et al., 2003), as having a major role in the arterial pole related defects. TBX1 has been shown to be required for outflow lengthening and final alignment in mice. Xu et al. (2004) used a tissue-specific knockout of Tbx1 in SHF to show that TBX1 is required for normal proliferation in the SHF. Reduced proliferation in the SHF led to contribution of fewer myocardial cells to the outflow myocardium from the SHF and resulted in arterial pole alignment defects similar to the ones reported for NCA.

Importantly, several studies have also suggested that TBX1 regulates the expression of *Fgf8* (Abu-Issa et al., 2002; Frank et al., 2002; Kochilas et al., 2002; Vitelli et al., 2002) and it is well established that *Fgf8* hypomorphic mice have similar arterial pole alignment defects to those seen after NCA (Abu-Issa et al., 2002; Frank et al., 2002). Inactivation of *Fgf8* in *Tbx1*-expressing cells results in a DiGeorge phenotype (Brown et al., 2004). Our data add to the growing body of evidence that proliferation in the SHF must be tightly regulated for the SHF to contribute myocardium to the outflow tract, and this contribution is required for normal arterial pole alignment. Even though FGF8 has been shown to be a mitogen, further studies will be necessary to determine if increased in proliferation in the SHF is a direct consequence of increased FGF8 signaling. In humans, when the aorta is positioned to the right of the pulmonary trunk, i.e. “dextroposed”, the defect is classified as overriding aorta. If the aorta overrides more than 50% it is classified as DORV. If the pulmonary trunk is smaller and the aorta is overriding, the defect is classified as tetralogy of Fallot. We have previously reported that malalignment defects are produced by NCA. However, this study and a recent one in which the right SHF was ablated (Ward et al., 2005), both show pulmonary stenosis and atresia. These two defects have never been seen after NCA which is limited to overriding aorta or DORV. Therefore, pulmonary stenosis or atresia as seen in tetralogy of Fallot is more likely due to abnormal addition of cells from the SHF and not to NCA. The pulmonary stenosis/atresia phenotype appears to be directly related to poor proliferation of the SHF and not excessive proliferation as is seen after NCA when Fgf8 signaling is also excessive.

This study and several earlier reports from our lab have shown that the myocardial calcium transient is reduced after NCA, and it was shown that anti-FGF8b can rescue the calcium transient in culture (Farrell et al., 2001). We now show that the calcium transient is also rescued in NCA embryos by reducing FGF8 signaling. We still do not fully understand the mechanism by which the myocardial function is depressed after NCA. Other studies have shown that FGF2 can repress the expression of the ryanodine receptor that mediates calcium release from the sarcoplasmic reticulum (Marks et al., 1991). FGF2 has also been shown to depress the myocardial calcium transient in cultured adult rat cardiomyocytes (Ishibashi et al., 1997). A recent study shows that periodic calcium activity, i.e. transients, elicited by FGF through activation of phospholipase C correlates temporally with the onset of gene expression in *Xenopus* embryos which suggests that there might be a causal relationship between calcium transients and gene expression (Diaz et al., 2005). Other FGFs are expressed in the myocardium and it is possible that levels of FGF8 signaling in the caudal pharynx affect myocardial FGF production.

The importance of CNC in arterial pole development takes two forms: direct and indirect. CNC form the outflow septation complex that is required for division of the outflow tract into systemic and pulmonary circulations (Kirby et al., 1983; Waldo et al., 1998). In addition, our study now shows that CNC modulate FGF8 signaling in the caudal pharynx during the temporal window when myocardial cells are added to the outflow tract from the SHF. Because the level of FGF8 signaling is critical for addition of these cells to the outflow tract, we believe that the role of CNC in modulating growth factor availability in the pharyngeal apparatus may impact widely on pharyngeal development in addition to the outflow tract. The next step is to identify the mechanism(s) that CNC use to affect this modulation and whether this signaling directly or indirectly affects the SHF. Studies are underway examining the potential role of natural FGF signaling antagonists, such as the Sprouty family of genes and Mkp3, generally expressed in tissues targeted by FGF ligands are to be examined in the SHF and pharynx. Sprouty1 and Sprouty2 are expressed in dissected SHF containing ventral pharynx of mouse and chick (unpublished data). Our quantitative PCR experiments show that many of the downstream targets of FGF signaling are normally present in the caudal pharynx and are elevated after neural crest ablation including the MKP3 which has been shown to be a negative regulator of FGF8 signaling (Kawakami et al., 2003). In the limb, Mkp3 expressed in the mesenchyme plays a key role in mediating the proliferative, anti-apoptotic signaling produced by apical

ectodermal ridge-derived FGF8 (Kawakami et al., 2003). Further studies are needed to determine the role of these FGF8 signaling antagonist in the addition of the SHF with too much or too little FGF signaling.

Our data add to the growing body of evidence that the proper addition of the myocardium from the SHF to the looping heart tube is necessary for final arterial pole alignment, and that different regions and cell types in the caudal pharynx require different levels of FGF8 signaling. For example, in the *Fgf8* hypomorphic mice, there is an increase in cell death in the neural crest, suggesting that CNC require high levels of FGF8 for normal development (Abu-Issa et al., 2002; Frank et al., 2002). However, we saw no direct effects of reducing FGF on cardiac neural crest cells in the pharynx or outflow tract when treated at early stages, this may reflect a transient reduction of FGF signaling rather than a continuous reduction of FGF8 as in the hypomorphic mice. The only defect in neural crest-derived structures we did observe was a thickening of the tunica media of the arch arteries.

In addition to levels of FGF8, the source of the FGF8 signal may also be important. In mouse and chick, the FGF8 has been shown to be critical for early stages of cardiac mesoderm formation. In the mouse, FGF8 is expressed in the cardiogenic mesoderm (E7.75–E8.0) as well as the underlying inducing endoderm whereas in the chick it is only expressed in the underlying endoderm (Crossley and Martin, 1995; Alsan and Schultheiss, 2002). This endodermal FGF8 expression in the chick has been shown to be important in combination with BMPs in inducing cardiogenic mesoderm. In the mouse, the FGF8 expression disappears in the cardiac tissue and is expressed in the lateral pharyngeal ectoderm and endoderm, although some investigators report low levels FGF8 expression in the SHF, outflow tract and primitive right ventricle in an FGF8lacZ reporter line (Erik Meyers personal communication). The stage which we applied the FGF8 antibody would not affect the earliest cardiogenic mesoderm but certainly would affect the cardiogenic mesoderm in the SHF. At these stages, the critical source of FGF8, lateral pharyngeal ectoderm and endoderm, is the same in the mouse and chick. Some studies in the mouse have begun to address which the source of FGF8 is critical for which developmetal processes. In the mouse, tissue-specific ablation of *Fgf8* in the pharyngeal arch ectoderm results in arch artery patterning defects but no arterial pole defects (Macatee et al., 2003). The same study also reported a tissue-specific ablation of FGF8 in the endoderm and ectoderm and these mice had low incidence of aortic valve and coronary artery patterning defects (Macatee et al., 2003). However, the timing of this knockout is later than the ectodermal knockout and may only affect the smooth muscle component of the SHF. A third tissue-specific knockout of FGF8 using a Tbx1Cre ablated FGF8 from the early cardiogenic mesoderm and endoderm (but not the ectoderm) caused outflow defects (Brown et al., 2004). This suggests that the FGF8 produced by the pharyngeal endoderm may be more important for normal outflow development but final judgment about the specificity and timing of different sources of FGF8 signaling must be tested in other ways.

Acknowledgments

We thank Joyce Newton, Emily Antoon, Mary Ann Nyc and Sandy Parran for their assistance with histology. Supported by PHS grants HL36059, HL70140 and HD39946.

Appendix A. Supplementary data

Supplementary data associated with this article can be found, in the online version, at doi:10.1016/j.ydbio.2006.02.052.

References

Abu-Issa, R., Smyth, G., Smoak, I., Yamamura, K.-I., Meyers, E., 2002. Fgf8 is required for pharyngeal arch and cardiovascular development in the mouse. Development 129, 4613–4625.

Alsan, B.H., Schultheiss, T.M., 2002. Regulation of avian cardiogenesis by Fgf8 signaling. Development 8, 1935–1943.

Basilico, C., Moscatelli, D., 1992. The FGF family of growth factors and oncogenes. Adv. Cancer Res. 59, 115–165.

Brown, C.B., Wenning, J.M., Lu, M.M., Epstein, D.J., Meyers, E.N., Epstein, J.A., 2004. Cre-mediated excision of Fgf8 in the Tbx1 expression domain reveals a critical role for Fgf8 in cardiovascular development in the mouse. Dev. Biol. 267, 190–202.

Creazzo, T.L., Brotto, M.A., Burch, J., 1997. Excitation–contraction coupling in the day 15 embryonic chick heart with persistent truncus arteriosus. Pediatr. Res. 42, 731–737.

Creazzo, T.L., Burch, J., Godt, R.E., 2004. Calcium buffering and excitation–contraction coupling in developing avian myocardium. Biophys. J. 86, 966–977.

Crossley, P.H., Martin, G.R., 1995. The mouse Fgf8 gene encodes a family of polypeptides and is expressed in regions that direct outgrowth and patterning in the developing embryo. Development 121, 439–451.

Crossley, P.H., Minowada, G., MacArthur, C.A., Martin, G.R., 1996. Roles for FGF8 in the induction, initiation, and maintenance of chick limb development. Cell 84, 127–136.

Diaz, J., Pastor, N., Martinez-Mekler, G., 2005. Role of a spatial distribution of IP3 receptors in the Ca2+ dynamics of the *Xenopus* embryo at the mid-blastula transition stage. Dev. Dyn. 232, 301–312.

Farrell, M.J., Burch, J.L., Wallis, K., Rowley, L., Kumiski, D., Stadt, H., Godt, R.E., Creazzo, T.L., Kirby, M.L., 2001. FGF-8 in the ventral pharynx alters development of myocardial calcium transients after neural crest ablation. J. Clin. Invest. 107, 1509–1517.

Frank, D., Fotheringham, L., Brewer, J., Muglia, L., Tristani-Firouzi, M., Capecchi, M.R., Moon, A., 2002. An Fgf8 mouse mutant phenocopies human 22q11 deletion syndrome. Development 129, 4591–4603.

Haworth, K.E., Healy, C., Sharpe, P.T., 2005. Characterization of the genomic structure of chick Fgf8. DNA Seq. 3, 180–186.

Hutson, M.R., Kirby, M.L., 2003. Neural crest and cardiovascular development: a 20-year perspective. Birth Defects Res. Part C Embryo Today 69, 2–13.

Ishibashi, Y., Urabe, Y., Tsutsui, H., Kinugawa, S., Sugimachi, M., Takahashi, M., Yamamoto, S., Tagawa, H., Sunagawa, K., Takeshita, A., 1997. Negative inotropic effect of basic fibroblast growth factor on adult rat cardiac myocyte. Circulation 96, 2501–2504.

Jerome, L.A., Papaioannou, V.E., 2001. DiGeorge syndrome phenotype in mice mutant for the T-box gene, Tbx1. Nat. Genet. 27, 286–291.

Kawakami, Y., Rodriguez-Leon, J., Koth, C.M., Buscher, D., Itoh, T., Raya, A., Ng, J.K., Esteban, C.R., Takahashi, S., Henrique, D., Schwarz, M.F., Asahara, H., Belmonte, J.C., 2003. MKP3 mediates the cellular response to FGF8 signalling in the vertebrate limb. Nat. Cell Biol. 6, 513–519.

Kelly, R.G., Brown, N.A., Buckingham, M.E., 2001. The arterial pole of the mouse heart forms from Fgf10-expressing cells in pharyngeal mesoderm. Dev. Cell 1, 435–440.

Kirby, M.L., Gale, T.F., Stewart, D.E., 1983. Neural crest cells contribute to normal aorticopulmonary septation. Science 220, 1059–1061.

Kochilas, L., Merscher-Gomez, S., Lu, M.M., Potluri, V., Liao, J., Kucherlapati, R., Morrow, B., Epstein, J.A., 2002. The role of neural crest during cardiac development in a mouse model of DiGeorge syndrome. Dev. Biol. 251, 157–166.

Kuratani, S.C., Kirby, M.L., 1992. Migration and distribution of circumpharyngeal crest cells in the chick embryo. Formation of the circumpharyngeal ridge and E/C8+ crest cells in the vertebrate head region. Anat. Rec. 234, 263–280.

Le Douarin, N.M., Dupin, E., Baroffio, A., Dulac, C., 1992. New insights into the development of neural crest derivatives. Int. Rev. Cytol. 138, 269–314.

Lindsay, E.A., Botta, A., Jurecic, V., Carattini-Rivera, S., Cheah, Y.C., Rosenblatt, H.M., Bradley, A., Baldini, A., 1999. Congenital heart disease in mice deficient for the DiGeorge syndrome region. Nature 401, 379–383.

Lindsay, E.A., Vitelli, F., Su, H., Morishima, M., Huynh, T., Pramparo, T., Jurecic, V., Ogunrinu, G., Sutherland, H.F., Scambler, P.J., Bradley, A., Baldini, A., 2001. Tbx1 haploinsufficieny in the DiGeorge syndrome region causes aortic arch defects in mice. Nature 410, 97–101.

Macatee, T.L., Hammond, B.P., Benjamin, R., Arenkiel, B.R., Francis, L., Frank, D.U., Moon, A.M., 2003. Ablation of specific expression domains reveals discrete functions of ectoderm- and endoderm-derived FGF8 during cardiovascular and pharyngeal development. Development 130, 6361–6374.

Mahmood, R., Bresnick, J., Hornbruch, A., Mahony, C., Morton, N., Colquhoun, K., Martin, P., Lumsden, A., Dickson, C., Mason, I., 1995. A role for FGF-8 in the initiation and maintenance of vertebrate limb bud outgrowth. Curr. Biol. 5, 797–806.

Marks, A.R., Taubman, M.B., Saito, A., Dai, Y., Fleischer, S., 1991. The ryanodine receptor/junctional channel complex is regulated by growth factors in a myogenic cell line. J. Cell Biol. 114, 303–312.

Martin, G., 2001. Making a vertebrate limb: new players enter from the wings. BioEssays 10, 865–868.

Merscher, S., Funke, B., Epstein, J.A., Heyer, J., Puech, A., Lu, M.M., Xavier, R.J., Demay, M.B., Russell, R.G., Factor, S., Tokooya, K., Jore, B.S., Lopez, M., Pandita, R.K., Lia, M., Carrion, D., Xu, H., Schorle, H., Kobler, J.B., Scambler, P., Wynshaw-Boris, A., Skoultchi, A.I., Morrow, B.E., Kucherlapati, R., 2001. TBX1 is responsible for cardiovascular defects in velo-cardio-facial/DiGeorge syndrome. Cell 104, 619–629.

Meyers, E.N., Lewandoski, M., Martin, G.R., 1998. An Fgf8 mutant allelic series generated by Cre- and Flp-mediated recombination. Nat. Genet. 18, 136–141.

Mjaatvedt, C.H., Nakaoka, T., Moreno-Rodriguez, R., Norris, R.A., Kern, M.J., Eisenberg, C.A., Turner, D., Markwald, R.R., 2001. The outflow tract of the heart is recruited from a novel heart-forming field. Dev. Biol. 238, 97–109.

Moon, A.M., Capecchi, M.R., 2000. Fgf8 is required for outgrowth and patterning of the limbs. Nat. Genet. 26, 455–459.

Olsen, S.K., Li, J.Y., Bromleigh, C., Eliseenkova, A.V., Ibrahimi, O.A., Lao, Z., Zhang, F., Linhardt, R.J., Joyner, A.L., Mohammadi, M., 2006. Structural basis by which alternative splicing modulates the organizer activity of FGF8 in the brain. Genes Dev. 20, 185–198.

Sato, T., Araki, I., Nakamura, H., 2001. Inductive signal and tissue responsiveness defining the tectum and the cerebellum. Development 128, 2461–2469.

Schneider, R.A., Hu, D., Rubenstein, J.L., Maden, M., Helms, J.A., 2001. Local retinoid signaling coordinates forebrain and facial morphogenesis by maintaining FGF8 and SHH. Development 128, 2755–2767.

Sun, X., Meyers, E.N., Lewandoski, M., Martin, G.R., 1999. Targeted disruption of Fgf8 causes failure of cell migration in the gastrulating mouse embryo. Genes Dev. 15, 1834–1846.

Vitelli, F., Taddei, I., Morishima, M., Meyers, E.N., Lindsay, E.A., Baldini, A., 2002. A genetic link between Tbx1 and fibroblast growth factor signaling. Development 129, 4605–4611.

Waldo, K.L., Kumiski, D., Kirby, M.L., 1996. Cardiac neural crest is essential for the persistence rather than the formation of an arch artery. Dev. Dyn. 20, 281–292.

Waldo, K., Miyagawa-Tomita, S., Kumiski, D., Kirby, M.L., 1998. Cardiac neural crest cells provide new insight into septation of the cardiac outflow tract: aortic sac to ventricular septal closure. Dev. Biol. 196, 129–144.

Waldo, K., Zdanowicz, M., Burch, J., Kumiski, D.H., Stadt, H.A., Godt, R.E., Creazzo, T.L., Kirby, M.L., 1999. A novel role for cardiac neural crest in heart development. J. Clin. Invest. 103, 1499–1507.

Waldo, K.L., Kumiski, D.H., Wallis, K.T., Stadt, H.A., Hutson, M.R., Platt, D.H., Kirby, M.L., 2001. Conotruncal myocardium arises from a secondary heart field. Development 128, 3179–3188.

Waldo, K.L., Hutson, M.R., Ward, C.C., Zdanowicz, M., Stadt, H.A., Kumiski, D., Abu-Issa, R., Kirby, M.L., 2005a. Secondary heart field contributes myocardium and smooth muscle to the arterial pole of the developing heart. Dev. Biol. 281, 78–90.

Waldo, K.L., Hutson, M.R., Zdanowicz, M., Stadt, H.A., Zdanowicz, J., Kirby, M.L., 2005b. Cardiac neural crest is necessary for normal addition of the myocardium to the arterial pole from the secondary heart field. Dev. Biol. 281, 66–77.

Ward, C.C., Stadt, H.A., Hutson, M.R., Kirby, M.L., 2005. Secondary heart field ablation results in arterial pole defects including pulmonary atresia. Dev. Biol. 284, 72–83.

Xu, H., Morishima, M., Wylie, J.N., Schwartz, R.J., Bruneau, B.G., Lindsay, E.A., Baldini, A., 2004. Tbx1 has a dual role in the morphogenesis of the cardiac outflow tract. Development 131, 3217–3227.

Yagi, H., Furutani, Y., Hamada, H., Sasaki, T., Asakawa, S., Minoshima, S., Ichida, F., Joo, K., Kimura, M., Imamura, S., et al., 2003. Role of TBX1 in human del22q11.2 syndrome. Lancet 362, 1366–1373.

Yelbuz, T.M., Waldo, K.L., Kumiski, D.H., Stadt, H.A., Wolfe, R.R., Leatherbury, L., Kirby, M.L., 2002. Shortened outflow tract leads to altered cardiac looping after neural crest ablation. Circulation 106, 504–510.

Yelbuz, T.M., Waldo, K.L., Zhang, X.W., Zdanowicz, M., Parker, J., Creazzo, T.L., Johnson, G.A., Kirby, M.L., 2003. Myocardial volume and organization are changed by failure of addition of secondary heart field myocardium to the cardiac outflow tract. Dev. Dyn. 228, 152–160.